Study of the Structure−Properties Relationship of Phenolic Molecular Glass Resists for Next Generation Photolithography

Anuja De Silva,[†] Jin-Kyun Lee,[‡] Xavier André,[‡] Nelson M. Felix,[§] Heidi B. Cao,[△] Hai Deng,[△] and Christopher K. Ober*[,‡]

Department of Chemistry and Chemical Biology, Department of Materials Science and Engineering, and Department of Chemical and Biomolecular Engineering, Cornell University, Ithaca, New York 14850, and Intel Corp., 5200 N.E. Elam Young Parkway, Hillsborough, Oregon 97124

Received September 12, 2007. Revised Manuscript Received November 1, 2007

In this paper, we report the synthesis and characterization of a family of phenolic molecular glasses with variable size and branch architecture. This research is aimed at providing an improved understanding of the relationship between the structural variations of these phenolic photoresist materials and their thermal properties. In particular, the effects of the molecular weight, intermolecular hydrogen bonding, and structural effects on the glass transition temperature are studied in detail to gain a better understanding of their glass forming behavior. A fundamental understanding of such behavior is invaluable to the development of potential molecular photoresists for next generation lithography. Finally, these compounds are evaluated as positive-tone photoresists for lithographic applications for extreme UV ($\lambda = 13.4$ nm) lithography.

Introduction

Advances in next generation lithography as well as in optoelectronic technologies have increased interest in small, glass forming molecules. Such small molecules termed "molecular glasses" (MGs) possess structural features that inhibit crystallization and display high glass transition temperatures (Tg's) despite their modest size. MGs combine characteristic properties of small molecules, such as high purity and well defined structure, with beneficial aspects of polymers, such as high thermal stability and thin film forming properties. These molecules can be characterized by the presence of significant free volume and by disorder in both intermolecular distance and orientation.[1]The MG concept has been explored in a growing family of charge transport materials to circumvent several issues faced by polymer matrixes such as grain boundaries of various sizes that cause structural defects and deep carrier traps, chain entanglement, aging, and poor miscibility with small molecule chromophores.[2–5]

As the semiconductor industry moves to 32 nm feature sizes and below, obtaining smaller feature sizes with reduced fluctuations on the resist pattern, known as line edge roughness (LER), is a major focus.[6] Extensive investigations have shown that the possible limitations to resolution and the sources for LER are both material and process dependent.[7–9] Photoresist (or resist) polymer molecular weight, molecular weight distribution (MWD),[10,11] and polymer aggregation[12] are the main contributions to the poor lithographic performance of a given material. With MG resists, the resist building block may be as much as an order of magnitude in size smaller and may be monodisperse compared to conventional polymeric resists. The reduction of the "pixel" size is believed to be a fundamental improvement in the ability to consistently obtain high-resolution patterns. Theoretical studies have also shown that LER decreases with reduced molecular weight of the photoresist, both for classical and chemically amplified photoresists. The radius of gyration (Rg) of a photoresist polymer has also been directly correlated to LER. A smaller Rg can therefore consistently yield a smaller LER.[13,14]

To capitalize on the potential of MG photoresists, several structural requirements need to be fulfilled. The ability to demonstrate high Tg's compared to polymeric resist is a primary concern. Tg is an important factor in the ability to form stable thin films and to undergo several processing steps such as post-exposure bake (PEB), base development, and

* Corresponding author. E-mail: cober@ccmr.cornell.edu.
[†] Department of Chemistry and Chemical Biology.
[‡] Department of Materials Science and Engineering.
[§] Department of Chemical and Biomolecular Engineering.
[△] Intel Corp.

(1) Thorpe, M. F.; Tichy, L. *Properties and applications of amorphous materials*; Kluwer Academic Publishers: Dordrecht, 2001.
(2) Strohriegel, P.; Grazulevicius, J. V. *Adv. Mater.* **2002**, *14* (20), 1439–1452.
(3) Grazulevicius, J. V. *Polym. Adv. Technol.* **2006**, *17*, 694–696.
(4) Shirota, Y. *J. Mater. Chem.* **2005**, *15*, 75–93.
(5) Thelakkat, M.; Schmidt, H.-W. *Polym. Adv. Technol.* **1998**, *9* (7), 429–442.
(6) Cao, H.; Yueh, W.; Rice, B.; Roberts, J.; Bacuita, T.; Chandhok, M. *Adv. Resist Technol. Process. XXI* **2004**, *5376*, 757–763.
(7) Rau, N.; Ogawa, T.; Neureuther, A.; Kubena, R.; Willson, G. *J. Vac. Sci. Technol., B* **1998**, *16* (6), 3784–3788.
(8) Shin, J.; Han, G.; Ma, Y.; Moloni, K.; Cerrina, F. *J. Vac. Sci. Technol., B* **2001**, *19* (6), 2890–2895.
(9) Fedynyshyn, T. H.; Pottebaum, I.; Astolfi, D. K.; Cabral, A.; Roberts, J.; Meagley, A. R. *J. Vac. Sci. Technol., B* **2006**, *24* (6), 3031–3039.
(10) Shiraishi, H.; Yoshimura, T.; Sakamizu, T.; Ueno, T.; Okazaki, S. *J. Vac. Sci. Technol., B* **1994**, *12* (6), 3895–3899.
(11) Yoshimura, T.; Shiraishi, H.; Yamamoto, J.; Okazaki, S. *Appl. Phys. Lett.* **1993**, *63* (6), 764–766.
(12) Yamaguchi, T.; Namatsu, H.; Nagase, M.; Yamazaki, K.; Kurihara, K. *Appl. Phys. Lett.* **1997**, *71* (16), 2388–2390.
(13) Patsis, G. P.; Constantoudis, V.; Gogolides, E. *Microelectron. Eng.* **2004**, *75*, 297–308.
(14) Patsis, G. P.; Gogolides, E. *Microelectron. Eng.* **2006**, *83*, 1078–1081.

10.1021/cm702613n CCC: $40.75
Published on Web 01/03/2008

etching. The PEB step is essential to resist processing as it provides the thermal energy needed to enable acid catalyzed deprotection for positive tone or cross-linking for negative tone resists. For successful processing, the resist material must be used below its Tg. Performing the PEB at a temperature above the Tg of the material can have adverse effects in limiting resolution, pattern distortion, and promoting acid diffusion during PEB. As in MG photoresists, Tg is also a crucial factor in charge transport amorphous materials. It has been reported that high Tg has been directly correlated to high electroluminescence stability.[15]

Several approaches taken to design stable MGs have been discussed in detail in the literature.[15–20] According to the Tammann rule,[21] all substances in nature can be transformed into the glassy state below their melting temperatures. However in most cases, because of a strong tendency toward crystallization at temperatures between the melting point and Tg, the glassy state cannot be reached. The stability of the amorphous phase in a small molecule can be explained by the crystal growth velocity, which is a kinetic parameter related to the transition from amorphous to the crystalline phase.[16,17] High maximum crystal growth temperature and low minimum crystal growth velocity are required for stable amorphous states of small organic materials. A first approach to designing MG materials has been to include features with nonplanar irregular shapes that inhibit crystallization.[19,22] Molecules that are able to exist in a large number of different conformations with almost equal conformational energies should possess a weakened tendency toward crystallization for kinetic reasons.[23,24] Molecular geometry also plays a crucial role in the glass forming ability of molecular systems. Common glass forming topologies include branched or star shapes,[25–29] spiro links,[30,31] tetrahedral,[32,33] and twin molecular structures.[34,35] The stability of the glassy phase also increases with enlargement of the molecular size.[17,18] The molecular architecture is important in creating a dense, bulky molecular system with a high tendency toward vitrification.

When designing amorphous molecular materials, structural features that increase Tg in addition to reducing crystal growth rate must be incorporated. Though asymmetric structures seem more conducive to glass formation as a result of difficulties in molecular packing, they can also lower Tg by increasing free volume. Hence, a careful balance needs to be reached when incorporating structural moieties that can form a stable glass as well as demonstrate a high Tg. The glass transition of MGs is considered to be the temperature at which a dramatic free volume increase occurs, and molecular motions that are caused by intramolecular bond rotation take place resulting in a change in their position of equilibrium. Structural features that decrease free volume and restrict rotation about any molecular axis are expected to raise Tg. Inclusion of rigid and bulky groups such as *tert*-butyl, biphenyl, and fluorene moieties increases Tg by hindering the translational, rotational, and vibrational motions of the molecule.[36,37] The presence of intermolecular interactions, such as dipole–dipole and hydrogen bonding interactions, has the ability to increase Tg by decreasing the free volume. These fundamental concepts have been applied to forming several thermally stable inorganic and organic systems with high Tg's. Our design strategy for patternable MGs is also based on many of these guidelines that favor the formation of amorphous materials combined with good photoresist performance.

As a point of reference, it is worthwhile first to consider the polymeric photoresists. Poly(4-hydroxy styrene) (PHS) based polymers have shown great promise as extreme ultraviolet (EUV) resist materials. The phenolic component provides high Tg, etch resistance, and base solubility as a result of the presence of the phenolic groups that can be modified with a solubility switching functionality. On the basis of these attributes, phenolic MG resists are being developed as a versatile platform for next generation lithography. Phenolic compounds have potential as both chemically amplified negative and chemically amplified positive tone photoresist materials. The hydroxyl containing core structures can be used as negative tone photoresists with the addition of a cross-linking agent. With increasing size, these phenolic compounds demonstrate Tg's of a metastable state that can be compared to commercially available PHS (8k). The effect of the core structure is evaluated by changing between a planar benzene ring and a tetrahedral core design. Generally, an increase in glass transition with increasing molar mass is observed. In this paper, the effects of various structural links between phenyl rings and different isomeric states on the thermal properties of these phenolic compounds

(15) Shizuo, T.; Hiromitsu, T.; Koji, N.; Akane, O.; Yasunori, T. *Appl. Phys. Lett.* **1997**, *70* (15), 1929–1931.
(16) Naito, K.; Miura, A. *J. Phys. Chem.* **1991**, *97*, 6240–6248.
(17) Naito, K. *Chem. Mater.* **1994**, *6*, 2343–2350.
(18) Shirota, Y. *J. Mater. Chem.* **2000**, *10*, 1–25.
(19) Alig, I.; Braun, D.; Langendorf, R.; Wirth, H. O.; Voigt, M. H.; Wendorff, J. *J. Mater. Chem.* **1998**, *8* (4), 847–851.
(20) Wedler, W.; Demus, D.; Zaschke, H.; Mohr, K.; Schafer, W.; Weissflog, W. *J. Mater. Chem.* **1991**, *1* (3), 347–356.
(21) Tammann, G. *The State of Aggregation*, 2nd ed.; Van Nostrand: New York, 1925.
(22) Inada, H.; Ohnishi, K.; Nomura, S.; Higuchi, A.; Nakano, H.; Shirota, Y. *J. Mater. Chem.* **1994**, *4* (2), 171–177.
(23) Ishikawa, W.; Inada, H.; Nakano, H.; Shirota, Y. *Chem. Lett.* **1991**, *10*, 1731–1734.
(24) Ueta, E.; Nakano, H.; Shirota, Y. *Chem. Lett.* **1994**, *12*, 2397–2400.
(25) Bettenhausen, J.; Strohriegl, P. *Adv. Mater.* **1996**, *8* (6), 507–510.
(26) Sonntag, M.; Kreger, K.; Hanft, D.; Strohriegl, P. *Chem. Mater.* **2005**, *17*, 3031–3039.
(27) Higuchi, A.; Inada, H.; Kobata, T.; Shirota, Y. *Adv. Mater.* **1991**, *3* (11), 549–550.
(28) Ishikawa, W.; Noguchi, K.; Kuwabara, Y.; Shirota, Y. *Adv. Mater.* **1993**, *5* (7–8), 559–561.
(29) Kuwabara, Y.; Ogawa, H.; Inada, H.; Noma, N.; Shirota, Y. *Adv. Mater.* **1994**, *6* (9), 677–679.
(30) Steuber, B. F.; Staudigel, J.; Stössel, M.; Simmerer, J.; Winnacker, A.; Spreitzer, H.; Weissörtel, F.; Salbeck, J. *Adv. Mater.* **2000**, *12* (2), 130–133.
(31) Johansson, N.; Salbeck, J.; Bauer, J.; Weissörtel, F.; Bröms, P.; Andersson, A.; Salaneck, W. R. *Adv. Mater.* **1998**, *10* (14), 1136–1141.
(32) Wang, S., Jr.; Raymond, A.; Hudack, J.; Bazan, G. C. *J. Am. Chem. Soc.* **2000**, *122*, 5695–5709.
(33) Reichert, V. R.; Mathias, L. J. *Macromolecules* **1994**, *27*, 7015–7023.
(34) Grigalevicius, S.; Blazys, G.; Ostrauskaite, J.; Grazulevicius, J. V.; Gaidelis, V.; Jankauskas, V. *J. Photochem. Photobiol., A* **2003**, *154*, 161–167.
(35) Theissen, U.; Zilker, S. J.; Pfeuffer, T.; Strohriegl, P. *Adv. Mater.* **2000**, *12* (22), 1698–1700.
(36) Liu, X.-M.; He, C.; Huang, J.; Xu, J. *Chem. Mater.* **2005**, *17*, 434–441.
(37) Okumoto, K.; Wayaku, K.; Noda, T.; Kageyama, H.; Shirota, Y. *Synth. Met.* **2000**, *111–112*, 473–476.

are studied in detail to gain a better understanding of the glass forming phenomena. Positive tone MG photoresists were synthesized by protecting the hydroxyl moieties with acid labile *tert*-butyl carbonate (*t*-BOC) protecting groups with partial (approximately 50%) and complete degrees of protection. This paper also explores the effect of factors that affect Tg in protected compounds as a result of the interplay of mass increase, molecular architecture, and intermolecular hydrogen bonding.

Experimental Section

Materials. Chemicals were purchased from Sigma-Aldrich unless otherwise stated and were used without further purification. Anhydrous or high-performance liquid chromatography (HPLC) grade solvents were used unless otherwise stated. Commercially available AZ 300 MIF was employed as a standard developer (0.26 N tetramethylammonium hydroxide in water, TMAH).

Characterization. ^{1}H NMR spectra were recorded on a Varian Inova-400 (400 MHz) or Inova-500 (500 MHz) spectrometer at room temperature, using the chemical shift of a residual protic solvent ($CHCl_3$ at δ 7.28 ppm, acetone at 2.05 ppm, or dimethyl sulfoxide (DMSO) at δ 2.50 ppm) as an internal reference. All shifts are quoted in parts per million (ppm) relative to $CHCl_3$, acetone, or DMSO, and coupling constants J are measured in hertz. The multiplicity of the signal is indicated as follows: s (singlet), d (doublet), t (triplet), q (quartet), m (multiplet), dd (doublet of doublets), dt (doublet of triplets), dm (doublet of multiplets), and br s (broad singlet). ^{13}C NMR spectra were recorded on a Varian Inova-400 (100 MHz) or Inova-500 (125 MHz) spectrometer using the central resonance of the triplet of $CDCl_3$ at δ 77.0 ppm or using the central resonance of the septuplet of DMSO-d_6 at 40.0 ppm as an internal reference. Fourier transform infared (FT-IR) spectra were recorded on a Mattson Instruments Galaxy 2020 FT-IR spectrometer. Thermogravimetric analysis (TGA) was performed on a TA Instruments Q500 at a heating rate of 10 °C/min under N_2. The Tg of resist materials was measured on a TA Instruments Q1000 modulated differential scanning calorimeter at a heat/cool rate of 10 °C/min under N_2 for three heat/cool cycles. Tg was determined from the second heating/cooling cycle.

Powder X-ray diffraction (PXRD) traces were obtained using a Scintag Theta-Theta XDS2000 diffractometer to examine the crystallinity of the bulk material.

Lithographic Evaluation of Positive-Tone MGs. The resist compounds were dissolved in propylene glycol methyl ether acetate (PGMEA) making a 5 wt % solution. A commercially available photoacid generator (PAG), triphenylsulfonium perfluoro-1-butanesulfonate (5% with respect to resist), and trioctylamine (0.3 wt % with respect to resist) were added, and the solution was filtered through a 0.2 mm membrane filter. Then, the solutions were spin coated onto a 4 in. HMDS primed silicon wafer (2000 rpm, 30 s) leading to approximately 100 nm thick films. This was subjected to a post-application bake at 130 °C for 60 s, then exposed using EUV radiation. After exposure, the wafer was baked at 80 °C for 30 s and then developed in an aqueous solution of AZ 300 MIF developer (0.262 N TMAH) for 20 s.

Metrology. Scanning electron micrographs (SEMs) were taken on a Zeiss Ultra 55 scanning electron microscope. LER was calculated using SuMMIT (EUV Technology) image analysis software. An SEM image of a 100 nm line/space pattern was taken for each line edge. The LER value was the average of 10 adjacent lines.

Synthesis of Phenolic MGs. The general synthetic procedure for phenolic MGs is described with the synthesis of CR6 given in detail as a representative. CR1−CR10 were prepared using similar synthetic procedures with their respective ketone or aldehyde. α,α,α′-tris(4-hydroxyphenyl)-1-ethyl-4-isopropylbenzene (CR7) was purchased from TCI America and used without further purification.

CR6. To a magnetically stirred solution of 1,1,1-tris(4-acetylphenyl)ethane (**25**)[38] (7.46 g, 19.4 mmol) and phenol (43.8 g, 466 mmol) in acetic acid (45 cm^3) was added hydrochloric acid (12 M aqueous solution, 135 cm^3) at room temperature. The solution was stirred for 48 h at 90 °C and then cooled to room temperature. The solid precipitated on the bottom was recovered, washed with a copious amount of water, and dissolved in EtOAc (100 cm^3). The organic solution was washed with brine (100 cm^3), dried over anhydrous $MgSO_4$, passed through a short plug of silica gel, and then concentrated under reduced pressure. CH_2Cl_2 (150 cm^3) was added to precipitate a crude product. The filtered solid was further purified by flash column chromatography (silica gel, THF/hexane 1:1 to 2:1) to give CR6 (**26**) as a pale-yellow solid (1.89 g, yield = 11%); IR (KBr pellet) ν_{max} 3384 (br), 3033, 2980, 1609, 1511, 1437, 1374, 1234, 1178, 1069, 1016, 834 cm^{-1}. ^{1}H NMR (500 MHz, DMSO-d_6): δ = 1.97 (s, 9H, 3 × CH_3), 2.03 (s, 3H, CH_3), 6.63 (d, J = 8 Hz, 12H, Ar−H), 6.81 (d, J = 8 Hz, 12H, Ar−H), 6.90 (s, 12H, Ar−H), 9.24 ppm (br s, 6H, 6 × Ar−OH). ^{13}C NMR (125 MHz, DMSO-d_6): δ = 30.5, 30.8, 50.8, 51.5, 115.0, 128.1, 128.2, 129.7, 140.1, 146.5, 147.8, 155.6 ppm. MALDI calcd for (M + Na)$^+$, 917.39; found, 917.43.

CR1. Yield = 42%; IR (KBr pellet) ν_{max} 3354 (br), 3042, 2983, 1888, 1700, 1610, 1508, 1443, 1370, 1244, 1182, 1115, 1021, 830, 704 cm^{-1}. ^{1}H NMR (500 MHz, DMSO-d_6): δ = 1.89 (s, 3H, CH_3), 6.64 (d, J = 7.9 Hz, 4H, Ar−H), 6.8 (d, J = 8 Hz, 4H, Ar−H), 7.00 (d, J = 8.3 Hz, 2H, Ar−H), 7.16 (t, J = 7.3 Hz, 1H, Ar−H), 7.24 (t, J = 7.7 Hz, 2H, Ar−H), 9.25 ppm (br s, 2H, 2 × Ar−OH). ^{13}C NMR (125 MHz, DMSO-d_6): δ = 30.8, 51.17, 115.00, 126.15, 128.24, 128.76, 129.75, 140.03, 150.42, 155.71 ppm. Anal. Calcd for $C_{20}H_{18}O_2$: C, 82.73; H, 6.25. Found: C, 82.64; H, 6.34.

CR2. Yield = 92%; IR (KBr pellet) ν_{max} 3376 (br), 2976, 1653, 1596, 1510, 1432, 1376, 1235, 1177, 1116, 1014, 832, 711 cm^{-1}. ^{1}H NMR (500 MHz, DMSO-d_6): δ = 1.89 (s, 6H, 2 × CH_3), 6.60 (d, J = 8.2 Hz, 8H, Ar−H), 6.74 (d, J = 8.4 Hz, 8H, Ar−H), 6.9 (s, 1H, Ar−H), 7.08 (s, 1H, Ar−H), 9.35 ppm (br s, 6H, 4 × Ar−OH). ^{13}C NMR (125 MHz, DMSO-d_6): δ = 30.8, 51.3, 114.9, 125.8, 129.7, 140.22, 149.5, 155.6 ppm. MALDI calcd for (M + Na)$^+$, 525.21; found, 525.26. Anal. Calcd for $C_{30}H_{34}O_4$: C, 81.25; H, 6.02. Found: C, 81.58; H, 6.23.

CR3. Yield = 85%; IR (KBr pellet) ν_{max} 3358 (br), 2975, 2362, 1891, 1611, 1512, 1435, 1374, 1239, 1177, 1013, 891, 832 cm^{-1}. ^{1}H NMR (500 MHz, DMSO-d_6): δ = 1.76 (s, 9H, 3 × CH_3), 6.55 (d, J = 8.4 Hz, 12H, Ar−H), 6.62 (s, 12H, Ar−H), 6.67 (d, J = 8.5 Hz, 12H, Ar−H), 9.27 ppm (br s, 6H, 6 × Ar−OH). ^{13}C NMR (125 MHz, DMSO-d_6): δ = 30.7, 51.3, 114.8, 126.6, 129.6, 140.2, 148.4, 155.5 ppm. MALDI calcd for (M + Na)$^+$, 737.3; found, 737.42. Anal. Calcd for $C_{48}H_{42}O_6$: C, 80.65; H, 5.92. Found: C, 80.25; H, 5.91.

CR4. Yield = 42%; IR (KBr pellet) ν_{max} 3363 (br), 3032, 2963, 1612, 1510, 1441, 1365, 1234, 1176, 1111, 1056, 1016, 835 cm^{-1}. ^{1}H NMR (500 MHz, DMSO-d_6): δ = 1.24 [s, 9H, (CH_3)$_3$C], 1.98 (s, 3H, CH_3), 6.64 (d, J = 8.5 Hz, 4H, Ar−H), 6.81 (d, J = 8.5 Hz, 4H, Ar−H), 6.93 (d, J = 8.5 Hz, 2H, Ar−H), 7.25 (d, J = 8.5 Hz, 2H, Ar−H), 9.27 ppm (br s, 2H, 2 × Ar−OH). ^{13}C NMR (125 MHz, DMSO-d_6): δ = 30.9, 31.7, 34.5, 50.8, 114.9, 124.9, 128.4, 129.7, 140.2, 147.3, 148.2, 155.6 ppm. MALDI calcd for (M − H)$^+$, 345.18; found, 345.04.

CR5. Yield = 29%; IR (KBr pellet) ν_{max} 3375 (br), 3028, 2971, 1610, 1509, 1434, 1370, 1263, 1231, 1177, 1113, 1088, 1016, 830

(38) Supplied in the Supporting Information.

cm^{-1}. ^{1}H NMR (500 MHz, DMSO-d_6): δ = 1.58 (s, 6H, 2 × CH_3), 1.97 (s, 6H, 2 × CH_3), 6.63 (d, J = 8.5 Hz, 8H, Ar−H), 6.80 (d, J = 8.5 Hz, 8H, Ar−H), 6.91 (d, J = 8.5 Hz, 4H, Ar−H), 7.10 (d, J = 8.5 Hz, 4H, Ar−H), 9.20 ppm (br s, 4H, 4 × Ar−OH). ^{13}C NMR (125 MHz, DMSO-d_6): δ = 30.8, 31.0, 42.1, 50.8, 114.9, 126.3, 128.3, 129.7, 140.1, 147.4, 147.7, 155.6 ppm. MALDI calcd for (M + Na)$^{+\cdot}$ 643.29; found, 643.33.

CR8. Yield = 90%; IR (KBr pellet) ν_{max} 3281 (br), 3026, 2978, 2941, 1894, 1610, 1593, 1510, 1435, 1372, 1298, 1223, 1180, 1117, 1012, 832, 595, 568 cm^{-1}. ^{1}H NMR (500 MHz, DMSO-d_6): δ = 1.97 (s, 6H, 2 × CH_3), 6.63 (d, J = 7.7 Hz, 8H, Ar−H), 6.80 (d, J = 7.7 Hz, 8H, Ar−H), 6.89 (s, 4H, Ar−H), 9.25 ppm (br s, 4H, 4 × Ar−OH). ^{13}C NMR (125 MHz, DMSO-d_6): δ = 30.8, 50.81, 114.97, 128.05, 129.70, 140.13, 147.44, 155.65 ppm. MALDI calcd for (M + Na)$^+$, 525.21; found, 525.23. Anal. Calcd for $C_{30}H_{34}O_4$: C, 81.25; H, 6.02. Found: C, 81.56; H, 6.23.

CR9. Yield = 88%; IR (KBr pellet) ν_{max} 3299 (br), 3029, 2975, 1897, 1710, 1610, 1594, 1511, 1432, 1392, 1222, 1178, 1114, 1064, 1041, 826, 729, 573 cm^{-1}. ^{1}H NMR (500 MHz, DMSO-d_6): δ = 2.03 (s, 6H, 2 × CH_3), 6.66 (d, J = 8.6 Hz, 8H, Ar−H), 6.84 (d, J = 8.6 Hz, 8H, Ar−H), 7.01 (d, J = 8.3 Hz, 4H, Ar−H), 7.53 (d, J = 8.3 Hz, 4H, Ar−H), 9.30 ppm (br s, 4H, 4 × Ar−OH). ^{13}C NMR (125 MHz, DMSO-d_6): δ = 30.8, 51.03, 115.09, 126.44, 129.34, 130.68, 137.67, 140.00, 149.54, 155.79 ppm. MALDI calcd for (M + Na)$^+$, 601.25; found, 601.28. Anal. Calcd for $C_{40}H_{34}O_4$: C, 83.02; H, 5.92. Found: C, 83.22; H, 6.27.

CR10. Yield = 24%; IR (KBr pellet) ν_{max} 3375 (br), 3025, 2978, 1702, 1607, 1505, 1435, 1365, 1230, 1185, 1114, 1052, 1013, 824 cm^{-1}. ^{1}H NMR (500 MHz, DMSO-d_6): δ = 1.97 (s, 6H, 2 × CH_3), 3.83 (s, 2H, 1 × CH_2), 6.63 (d, J = 8.1 Hz, 8H, Ar−H), 6.79 (d, J = 8.2 Hz, 8H, Ar−H), 6.91 (d, J = 7.8 Hz, 4H, Ar−H), 7.09 (d, J = 7.8 Hz, 4H, Ar−H), 9.23 ppm (br s, 4H, 4 × Ar−OH). ^{13}C NMR (125 MHz, DMSO-d_6): δ = 30.9, 50.91, 115.00, 128.56, 128.86, 129.74, 130.66, 138.92, 140.12, 148.08, 155.69 ppm. MALDI calcd for (M + Na)$^+$, 615.26; found, 615.293. Anal. Calcd for $C_{40}H_{34}O_4$: C, 83.02; H, 5.92. Found: C, 83.22; H, 6.27.

***t*-BOC Protection of Phenolic MGs.** All MG cores were partially (approximately 50%) and completely protected by *t*-BOC groups using procedures found in the literature.[39] To obtain very pure samples, partially protected compounds were subsequently subjected to column chromatography with acetone as the eluent. The 100% *t*-BOC protected samples were purified using dichloromethane as the eluent.

Results

Synthesis of Phenolic MGs. The synthesis of phenolic molecules was performed by the condensation of phenol with a ketone or aldehyde in the presence of hydrochloric and acetic acid.[40] By varying the aromatic core, several compounds were synthesized with increasing mass and phenolic content. The compounds were obtained in relatively moderate yields after careful purification with a combination of solvent mixtures. As a result of the small size of these phenolic compounds, regular chromatographic techniques could be used for purification. These compounds were protected with *t*-BOC to varying degrees (50−100%) by a standard base catalyzed reaction in the presence of 4-dimethyl amino pyridine.

(39) Hansen, M. M.; Riggs, J. R. *Tetrahedron Lett.* **1998**, *39*, 2705–2706.
(40) Iwane, H.; Sugawara, T.; Suzuki, N.; Kaneko, K.; Shirasaki, Y. *Jpn. Kokai Tokkyo Koho*, Japanese patent JP 04145039 A 19920519 Heisei, 1992. Patent written in Japanese, Application: JP 90-265135.

Scheme 1. Design of MG Series 1

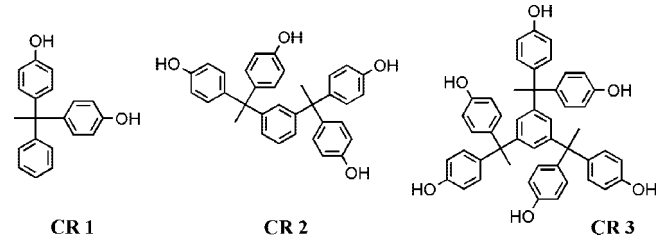

CR 1 CR 2 CR 3

The Series 1 (Scheme 1) is based on a systematic size increase of the branches around a planar benzene core. The commercial availability of acetophenone and its 1,3- and 1,3,5-derivatives enabled these compounds to be synthesized in a one step process.

In Series 2 (Scheme 2), the MG compounds were designed around a tetrahedral carbon center. The respective ketone precursors were synthesized under standard Friedel–Crafts acylation conditions with $AlCl_3$ and acetyl chloride.

Some additional compounds (Scheme 3) included in this discussion of phenolic MGs include commercially available CR7 and three other synthesized compounds (CR8−CR10).

Thermal Properties. The thermal properties of the phenolic MGs were investigated by differential scanning calorimetry (DSC) and TGA. The thermal stability and Tg of these compounds play a critical role in lithographic performance. High Tg and good thermal stability at elevated temperatures are prerequisites for their use in practical applications. Besides the small phenolic structures (MW < 350 g/mol), all other unprotected compounds demonstrate good thermal stability until about 300 °C. When partially protected with *t*-BOC groups, the thermal stability decreases up to about 130 °C whereas it is around 160 °C for fully protected compounds. Both unprotected and protected phenolic MGs exhibit Tg's significantly higher than room temperature.

MG Series 1. The first series was based on a systematic introduction of branches around a benzene core. The mass was increased in steps of 212 g/mol with addition of each branch. The smallest compound was crystalline as a result of its small size and compact shape. It was able to demonstrate thermal transitions corresponding to both crystalline and glassy phases. However, the larger molecules were amorphous as a result of the short arms that branch out from the 1, 3, and 5 positions of the benzene core. This starburst architecture, which forms a bulky structure with a low length to breath ratio of the molecule, was very conducive to glass formation. All three compounds (CR1–CR3) were amorphous in their partially and fully protected state. The partially protected compounds demonstrated higher Tg's than their fully protected counterparts, suggesting that intermolecular hydrogen bonding in the 50% protected samples was more dominant in increasing Tg than the increase in mass because of the 100% *t*-BOC protection. The complete characterization of the MG Series 1 is listed on Table 1.

MG Series 2. In the second series, the MG compounds were designed around a tetrahedral carbon atom. It has been reported that compounds branched from a central tetrahedral point of convergence have inherent glass forming ability[32,33]

Scheme 2. Design of MG Series 2

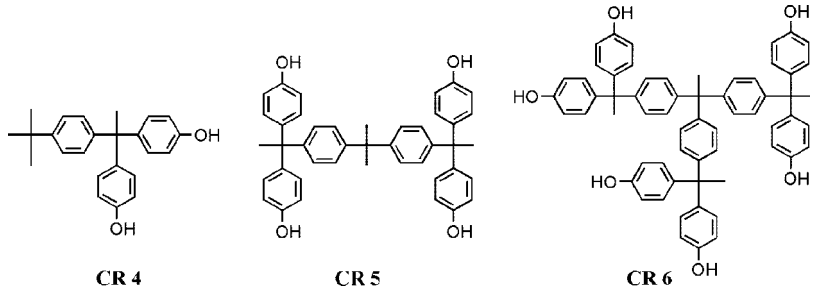

Scheme 3. Additional Compounds

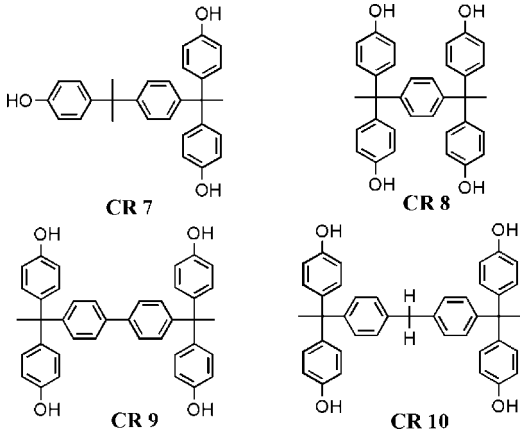

Table 1. Characterization of the MGs (Series 1)

MG compound	% of *t*-BOC protection[a]	phenolic function	MW (g/mol)	Tg[b] (°C)	C/O ratio
CR1-0	0	2	290.4	58	7.51
CR2-0	0	4	502.6	100	6.38
CR3-0	0	6	714.9	126	6
CR1-50	50	1	390.5	42	4.69
CR2-50	50	2	702.9	80	4.13
CR3-50	50	3	1015.2	94	3.94
CR1-100	100	0	490.6	33	3.75
CR2-100	100	0	903.1	74	3.38
CR3-100	100	0	1315.5	83	3.25

[a] CR1-50−CR3-50 denote approximately 50% *t*-BOC protected compound. [b] Tg obtained from from DSC, second heating cycle, 10 °C/min.

The smallest compound (CR4) was designed with a bulky *tert*-butyl group attached. Though the *tert*-butyl group increases the Tg of the unprotected compound, it enables crystallization in the fully protected state. Similarly, the methylethylidene link can increase Tg in the unprotected phenolic MG CR5 but also facilitates crystallization when fully protected with *t*-BOC. The crystalline tendencies of these compounds can be attributed to a better packing ability due to the methyl groups that extend from the sp^3 hybridized central carbon. The CR6 compound is the largest phenolic MG designed with a branched architecture in this series. In the partially protected state, the Tg of this series also scales with molecular weight similar to previous observations. But because of its large size and branched architecture, CR6 and its protected derivatives remain amorphous and show no difference in Tg between the partially and the fully protected. The complete characterization of the MG Series 2 is listed in Tables 1 and 2.

Table 2. Characterization of the MGs (Series 2)

MG compound	% of *t*-BOC protection[a]	phenolic function	MW (g/mol)	Tg[b] (°C)	C/O ratio
CR4-0	0	2	346.5	65	9
CR5-0	0	4	620.8	125	8.07
CR6-0	0	6	895.1	130	7.76
CR4-50	50	1	446.6	51	5.44
CR5-50	50	2	821	80	4.97
CR6-50	50	3	1195.5	129	4.82
CR4-100	100	0	546.7	no Tg	4.25
CR5-100	100	0	1021.4	no Tg	3.94
CR6-100	100	0	1495.8	129	3.84

[a] CR4-50−CR6-50 denote approximately 50% *t*-BOC protected compounds. [b] Tg obtained from from DSC, second heating cycle, 10 °C/min.

Discussion

1. Trends in Tg for Phenolic Compounds. This paper presents the characterization of a selected series of phenolic MGs (CR1−CR10) with increasing molecular size. Thermal analysis through DSC of the unprotected compounds shows that these materials yield kinetically trapped amorphous solids. These compounds can be vitrified upon cooling from the melt and demonstrate a Tg which can be confirmed through multiple heat/cool cycles. The reported temperature range for the Tg of a commercially available PHS is between 135 and 180 °C (effect of polydispersity). The Tg of a polymer is associated with long-range cooperative relaxation phenomena through large segmental motions. Any structural feature that increases segment size, chain stiffness, and intermolecular interactions can increase the Tg. Similarly, architecture plays a major role in MGs, especially in compensating for the modest sizes in MG structures. The rigid core and branched design are important features that increase segment size and decrease free volume in these molecules. Therefore, it is possible to obtain compounds of high Tg's with relatively modest masses compared to polymeric structures that are 1 order of magnitude larger in mass.

As shown in Figure 1, the Tg of phenolic MGs scale with molecular size, where the highest Tg of 130 °C is measured for the largest MG (CR6, MW = 895 g/mol). The thermal properties of unprotected MGs are also important in determining their viability as negative tone photoresists when combined with a cross-linker and a PAG. Additionally, the two fitted lines in Figure 1 indicate that the dependence of Tg on MW is more pronounced below ~700 g/mol. In the high-MW regime, the MGs consist of six or more hydroxyl groups and possess a Tg comparable to PHS despite their

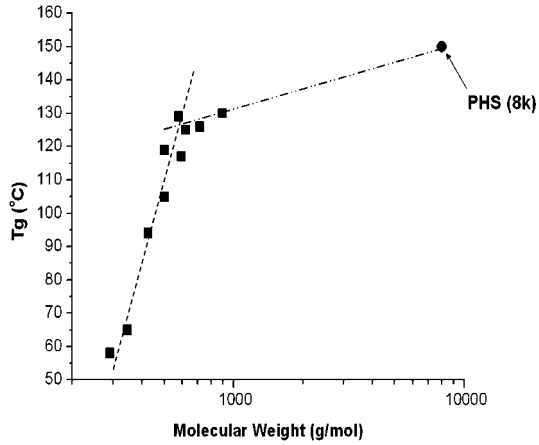

Figure 1. Evolution of the glass transition temperature with the molecular weight for the unprotected MGs.

modest size. It reveals that MGs are promising materials where the thermal properties can be tuned with more precision than for polymers.

Understanding the trends in the Tg of the phenolic MGs is important in determining their application as patterning materials. The unprotected phenolic molecules can be used as a component in a negative tone photoresist when combined with PAG and a cross-linking agent. Upon UV exposure, acid is generated in the PAG molecules, which causes an acid catalyzed cross-linking reaction during the PEB process in the exposed regions. The PEB step needs to be conducted at a sufficiently high temperature (usually above 90 °C) to form an extended network of phenolic MGs that remain insoluble under aqueous base conditions. The Tg of the phenolic material is important in controlling the PAG diffusion within the resist matrix during the PEB step. As the MG resists form a network through cross-linking, the Tg of the resist matrix is expected to increase, thus reinforcing the final pattern.

With the introduction of chemical amplification resist chemistry, the *t*-BOC group is widely used as a protecting group for positive tone resists.[41] These phenolic MG compounds can also be converted to positive tone resists through protection with *t*-BOC groups. Upon UV exposure, the PEB step (usually above 80 °C) is required to remove *t*-BOC groups through an acid catalyzed deprotection process. Similar to the negative tone system, understanding of the Tg of these protected MG compounds is crucial to their lithographic performance. Increased PAG diffusion can cause high LER and reduce pattern fidelity if PEB is conducted at a temperature higher than that of the resist Tg. Hence, a fundamental study of the factors that control the Tg of the *t*-BOC protected phenolic MGs is important for their potential application as next generation positive tone resist materials.

2. Trends in Tg for *t*-BOC Protected Phenolic Compounds. After protection with *t*-BOC and purification with column chromatography, many of these compounds formed amorphous solids after solvent evaporation. The Tg values

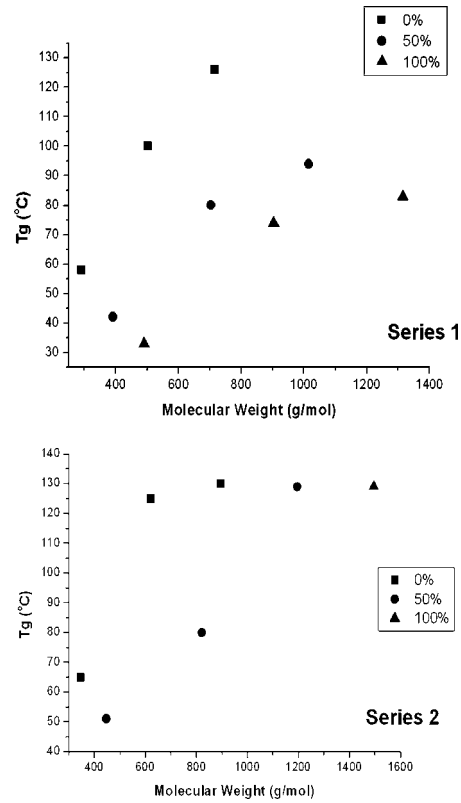

Figure 2. Effect of the *t*-Boc protection ratio on Tg for the MG compounds: Series 1 (top) and Series 2 (bottom).

of the partially and fully protected phenolic compounds are lower than those obtained for their unprotected counterparts (Figure 2). This behavior of the phenolic MGs, which is similar to that of PHS,[42] can be first attributed to the loss of the intermolecular hydrogen bonding with the introduction of the protecting groups.

Molecular size is a key factor in determining Tg's of protected MG resists as well. Within the Series 1 and 2, the Tg's of the partially and fully protected phenolic molecules scale with size. The increase in molecular size translates to an increase in the size of the segment of motion for each system. Therefore, the highest Tg for each series was demonstrated by the largest MG. A difference in MW of about 180 g/mol between the two larger phenolic MGs (CR3 and CR6) gives rise to a significant difference of 35 °C in the Tg for the partially protected MGs. But when fully protected, the Tg of CR3 is lowered while that of CR6 remains unchanged. At this size scale, the effect of increase in mass for the fully protected compound is comparable to the effect of hydrogen bonding between phenolic functional groups in the partially protected compound.

Most MGs used as positive tone resists are used in their partially protected state. The free hydroxyl groups in the resist system help with the solubility in spinning solvents and the adhesion to the silicon wafer. Furthermore, the sensitivity of the resist system increases and the miscibility of ionic small molecule PAGs is enhanced due to the polarity of the hydroxyl groups. The intermolecular hydrogen bonding

(41) Frechet, J. M. J.; Eichler, E.; Ito, H.; Willson, C. G. *Polymer* **1983**, *24* (8), 995–1000.

(42) Mertesdorf, C.; Falcigno, P.; Munzel, N.; Nathal, B.; Sehacht, H. T.; Zettler, A. *Polym. Mater. Sci. Eng.* **1995**, *72*, 147–148.

that occurs between the free hydroxyl groups also influences the Tg of the resist system. For most MGs, the partially protected systems display a higher Tg compared to that of their fully protected derivatives as a result of this effect. As the ability to form H-bonding per MG is proportional to the number of free phenolic functions, we can compare all phenolic MGs with four hydroxyl groups which are within the MW range of 703−821 g/mol. Partially protected MG resists (CR2-50, CR5-50, CR9-50, CR10-50) show Tg's around 80 °C despite the differences in their molecular architecture. As each of these molecules (approximately 45–55% *t*-BOC protection) has about two free hydroxyl groups, these systems can be expected to have similar hydrogen bonding characteristics. Within a comparable MW range, the Tg of partially protected phenolic MG resists is governed through the intermolecular hydrogen bonding.

In contrast, when fully protected with *t*-BOC groups, the structural features dominate the thermal behavior of these compounds. For MGs in the MW range of 703−821 g/mol discussed before, CR9 exhibits the highest Tg of 98 °C because of the rigid biphenyl core that restricts rotation about its molecular axis. CR10 has a lower Tg of 73 °C because of its flexible methylene linked core. CR5, with a methylethylidene link in its core, tends to crystallize when fully protected with *t*-BOC groups.

The isomeric effects on the glass forming ability can also be explored by comparing CR2 and CR8, which are 1,3 and 1,4 branched structures on a planar benzene core. CR8 has a higher Tg in its unprotected form as a result of its more linear structure enforced by the 1,4- para architecture that restricts rotation.[37] The Tg of CR2 is dependent on the intermolecular hydrogen bonding, and it crystallizes upon protection with *t*-BOC attributed to its highly symmetric structure. By inducing more planes of symmetry, the number of conformers formed is reduced as the tendency to crystallize is increased. But the 1,3-branched meta structure is very conducive to glass formation in any protected form.

Lithographic Evaluation

The first MG photoresist materials were introduced by Shirota et al. for electron beam lithography.[43,44] However, the doses required in e-beam exposure were 3 orders of magnitude higher than those typical for resists that decompose by chemically amplified acidolysis. By switching to chemically amplified MG resist systems, Shirota et al. were able to attain sub-100 nm feature sizes.[45] Shirota et al. also demonstrated that MGs with high Tg's showed higher sensitivity and resolution. Efforts from Ueda et al. investigated ring structures based on calix[4]resorcinarenes as the positive and negative tone resist systems.[46–48] Only micrometer sized features were obtained through a 365 nm exposure. Since then, several efforts have succeeded in producing MG photoresists with sub-50 nm capabilities.[49–52] A calix[4]resorcinarene derivative that produces 30 nm line space patterns under EUV (λ = 13.4 nm) conditions was developed by Chang et al., and this work represented the first report on sub-50 nm features obtained by an MG resist using standard processing conditions.[49] Our initial efforts on MGs were based on commercially available phenolic compounds such as CR7 and 5,5′,6,6′-tetrahydroxy-3,3,3′,3′-tetramethyl-1,1′-spirobisindane.[53] Patterns of 100 nm lines were obtained with electron beam lithography. When compared with the calix[4]resorcinarene resists that we have developed, the sub-100 °C glass transition was identified as a limiting factor for these phenolic resists to attain sub-50 nm features.

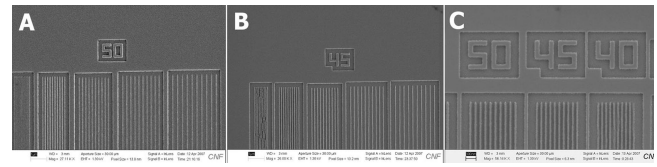

Figure 3. SEM images (sub-50 nm line/space) obtained after EUV exposure using (A) CR2-50, dose 18.5 mJ/cm^2, LER (3σ) 6.4 nm; (B) CR5-50, 5% PAG, dose 21.3 mJ/cm^2, LER (3σ) 5.5 nm; and (C) CR6-50, dose 25.6 mJ/cm^2, LER (3σ) 6.1 nm.

The goal of this systematic study of understanding the Tg behavior of the phenolic MGs is to develop high Tg resist systems. Several resist materials with Tg's of 80 °C or higher were identified as promising candidates capable of sub-50 nm resolution. For our initial lithographic assessment, three phenolic MG resists (CR2-50, CR5-50, CR6-50) were evaluated through EUV exposure at the Lawrence Berkeley National Laboratory (LBNL). The EUV microexposure tool at LBNL is capable of fabricating fine features below 30 nm. For all three compounds tested, the films were baked (i.e., PEB) at 75, 80, 85, and 90 °C for 30 s. The best result was obtained using a PEB of 80 °C. Although the PEB temperature was approximately equal to the Tg of this resist material for CR2-50 and CR5-50, sub-50 nm resolution was achieved (Figure 3). The highest resolution of 40 nm was obtained for CR6-50 which also exhibits the highest Tg resist system. These MG photoresist systems were developed in 0.26 N TMAH, which is the standard commercial developer.

As lower LER is expected to be a major advantage of MG resists compared with polymers, the LER values for the phenolic MG resists were evaluated using the SuMMIT image analysis software. LER values are measured from SEM images of 100 nm 1:1 line space patterns for each resist system. Studies on EUV polymeric resists that contain PHS

(43) Yoshiiwa, M.; Kageyama, H.; Shirota, Y.; Wakaya, F.; Gamo, K.; Takai, M. *Appl. Phys. Lett.* **1996**, *69* (17), 2605–2606.
(44) Kadota, T.; Kageyama, H.; Wakaya, F.; Gamo, K.; Shirota, Y. *Mater. Sci. Eng., C* **2001**, *16*, 91–94.
(45) Kadota, T.; Kageyama, H.; Wakaya, F.; Gamo, K.; Shirota, Y. *Chem. Lett.* **2004**, *33* (6), 706–707.
(46) Young-Gil, K.; Kim, J. B.; Fujigay, T.; Shibasaki, Y.; Ueda, M. *J. Mater. Chem.* **2002**, *12*, 53–57.
(47) Ueda, M.; Takahashi, D.; Nakayama, T.; Haba, O. *Chem. Mater.* **1998**, *10*, 2230–2234.
(48) Kamimura, Y.; Haba, O.; Endo, T.; Ueda, M. *J. Polym. Sci., Part A: Polym. Chem.* **2005**, *43*, 1210–1215.
(49) Chang, S. W.; Ayothi, R.; Bratto, D.; Yang, D.; Felix, N.; Cao, H. B.; Deng, H.; Ober, C. K. *J. Mater. Chem.* **2006**, *16*, 1470–1474.
(50) Felix, N. M.; Tsuchiya, K.; Ober, C. K. *Adv. Mater.* **2006**, *18*, 442–446.
(51) Hirayama, T.; Shiono, D.; Hada, H.; Onodera, J.; Ueda, M. *J. Photopolym. Sci. Technol.* **2004**, *17* (3), 435–440.
(52) Kojima, K.; Hattori, T.; Fukuda, H.; Hirayama, T.; Shiono, D.; Hada, H.; Onodera, J. *J. Photopolym. Sci. Technol.* **2006**, *19* (3), 373–378.
(53) Dai, J.; Chang, S. W.; Hamad, A.; Yang, D.; Felix, N.; Ober, C. K. *Chem. Mater.* **2006**, *18*, 3404–3411.

as a copolymer further demonstrate that the LER values obtained upon EUV exposure lie in the range of 9–12 nm.[8,54–56] The average LER values of these phenolic MG resist systems are below the average values obtained for polymeric systems. But even in MG resist systems, other material effects such as photoacid diffusion can negatively impact LER. This first set of results obtained shows that phenolic MG resists consistently demonstrate lower LER values compared to polymeric resists.

Conclusion

This study presents the complete synthesis and characterization of a library of small phenolic molecular resists. The structure–property relationship between molecular features and glass forming ability has been carefully investigated to establish some guidelines for phenolic MG resist design. Molecular weight, hydrogen bonding, and architecture effects on physical properties and photoresist performance have been examined through a family of phenolic compounds. Our work demonstrates that branched bulky architecture is conducive to forming high Tg resists with modest molecular weights. The change in Tg with different *t*-BOC protection ratios has also been evaluated to understand the use of these MGs as positive tone photoresists. Sub-50 nm features with reduced LER values of the MG resists were consistently less than those of polymeric resists when using EUV exposure. It is expected that further optimization of the experimental conditions will further reduce the pattern LER and provide a higher resolution of these phenolic MG systems in the future. These studies demonstrate the high potential of the phenolic MG photoresists for next generation lithography.

Acknowledgment. This work was funded by the Semiconductor Research Corporation (SRC) and the Intel Corporation. The authors would also like to thank Dr. Brian Hoef and Dr. Gideon Jones at Lawrence Berkeley Lab for EUV exposure and patterning. The Cornell Nanoscale Science and Technology Facility (CNF) and the Cornell Center for Materials Research (CCMR) are thanked for use of their facilities.

Supporting Information Available: Detailed synthesis and thermal characterization information (PDF). This material is available free of charge via the Internet at http://pubs.acs.org.

CM702613N

(54) Ma, Y.; Cheng, Y.-c.; Barwicz, T.; Smith, H. I.; Cerrina, F. *J. Vac. Sci. Technol., B* **2007**, *25* (1), 235–241.
(55) Ayothi, R.; Yi, Y.; Cao, H. B.; Yueh, W.; Putna, S.; Ober, C. K. *Chem. Mater.* **2007**, *19*, 1434–1444.
(56) Wang, M.; Gonsalves, K. E.; Rabinovich, M.; Yueh, W.; Roberts, J. M. *J. Mater. Chem.* **2007**, *17*, 1699–1706.